

RESEARCH PAPER



# LncUBE2R2-AS1 acts as a microRNA sponge of miR-302b to promote HCC progression via activation EGFR-PI3K-AKT signaling pathway

Zhe Wu, Zhi-Hong Wei, and Shao-Hua Chen

Department of Hepatology Surgery, 900 Hospital of the Joint Logistics Team, Fuzhou, Fujian, China

## ABSTRACT

Hepatocellular carcinoma (HCC) is a main cause of cancer-related deaths globally. Long non-coding RNAs (lncRNAs) play important roles in diverse cancers. LncRNA-UBE2R2-AS1 has been reported to promote apoptosis in glioma cell. However, the expressions, functions, and mechanisms of action of UBE2R2-AS1 in HCC are still unclear. UBE2R2-AS1 is increased in HCC tissues and cell lines. Increased expression of UBE2R2-AS1 is associated with large tumor size, multiple tumor number, advanced TNM stage, and poor survival of HCC patients. Functional experiments showed that knockdown UBE2R2-AS1 inhibited HCC growth and metastasis through in vitro and in vivo experiments. Regarding the mechanism, UBE2R2-AS1/miR-302b/EGFR established the ceRNA network involved in the modulation of cell progression of HCC cells via activation of PI3K-AKT signaling pathway. Overall, UBE2R2-AS1 may exhibit an oncogenic function in HCC via acting as a sponge for miR-302b to up-regulate EGFR, and may serve as a potential therapeutic target and a prognostic biomarker for HCC patients.

## ARTICLE HISTORY

Received 26 April 2020  
Revised 28 June 2020  
Accepted 10 July 2020

## KEYWORDS

HCC; UBE2R2-AS1; EGFR; PI3K-AKT; miR-302b

## Background

Hepatocellular carcinoma (HCC) was one of the biggest problems for human health worldwide [1], about 800,000 cases are diagnosed as HCC and over 850,000 deaths per year [2], however its pathogenesis still remains unclear [1]. Although several therapeutic methods developed, the HCC outcomes were still poor [3], with an approximately 30% 5-year survival rate [4]. Therefore, an urgent needed to further study the occurrence of HCC progression.

Long noncoding RNAs (lncRNAs) of a class of non-coding RNAs with longer than 200 nts in length, have exhibited the significant regulatory roles in the development of diverse pathologies and cancer types [5–7]. Various lncRNAs have been identified to exert roles in diagnosis [8], cell growth and metastasis [9,10], drug resistance [11], and therapy outcome prediction [12] in HCC. UBE2R2-AS1 was novelty lncRNA reported that promoted glioma cell apoptosis via targeting the miR-877-3p/TLR4 axis [13]. Nevertheless, the precise molecular mechanism of UBE2R2-AS1 in HCC was still largely vague. This study aimed to investigate the novelty mechanism of UBE2R2-AS1 in the progression of HCC.

## Methods

### *Patients and sample collection*

We analyzed 182 HCC tissues and their corresponding healthy tissue in samples collected from 900 Hospital of the Joint Logistics, Fuzhou, Fujian. The ethics committee of 900 Hospital of the Joint Logistics approved the study protocols and all participants provided informed consent. Patient information that could lead to patient identification remained confidential throughout the study. Patient demographics and clinical findings are listed in Table 1.

### *qRT-PCR analysis*

qRT-PCR assays were performed as previous analysis [14]. Briefly, total RNA was extracted from biopsies, plasma, and cells using TRIzol® reagent (Invitrogen; Thermo Fisher Scientific, Inc., Waltham, MA, USA). RT was performed using SuperScript III Reverse Transcriptase kit (Thermo Fisher Scientific, Inc.) to synthesize cDNA at following temperature conditions: 25°C for 5 min, 55°C for 15 min and 80°C for 10 min. SYBR-Green Real-Time PCR Master Mixes

**Table 1.** Association between UBE2R2-AS1 expression and clinicopathologic characteristics of 191 CRC patients in the study cohort.

Feature	UBE2R2-AS1		P-value
	High (N = 90)	Low (N = 91)	
<b>Age, y</b>			0.404
≥55	56	62	
<55	34	29	
<b>Gender</b>			0.393
Male	74	79	
Female	16	12	
<b>HBsAg</b>			0.503
Positive	81	79	
Negative	9	12	
<b>HBeAg</b>			0.272
Positive	66	73	
Negative	24	18	
<b>AFP, µg/L</b>			0.003
≥20	35	17	
<20	55	74	
<b>Tumor size, cm</b>			0.004
≥5	59	40	
<5	31	51	
<b>Tumor number</b>			0.043
Single	56	62	
Multiple	34	19	
<b>Vascular invasion</b>			0.505
Present	46	42	
Absent	44	49	
<b>Hepatitis B virus DNA, IU/mL</b>			0.206
≥1.0x10 <sup>3</sup>	43	35	
<1.0x10 <sup>3</sup>	47	56	
<b>Tumor differentiation</b>			0.211
I-II	6	11	
III	84	80	
<b>TNM stage</b>			0.001
I-II	53	74	
III	37	17	

The median UBE2R2-AS1 expression level served as the cutoff value to differentiate high and low expression groups (those above and below the 50<sup>th</sup> percentile). The correlation between UBE2R2-AS1 expression and patient clinical features was assessed via chi-squared tests.  $P < 0.05$  was the significance threshold.

(Thermo Fisher Scientific, Inc.) was used to prepare all PCR reactions. The PCR reaction conditions were 95°C for 1 min, followed by 40 cycles of 95°C for 10 sec and 60°C for 40 sec. Primers were all purchased from RiboBio (Guangzhou, China)

### Cell-based assays

Non-cancer cells (THLE-3) and HCC cell lines (Huh7, HepG2, MHCC-97H, and Hep3B) were grown in complete culture media (DMEM plus 10% FBS at 37°C, 5% CO<sub>2</sub>). For all mentioned

transfection reagents were obtained by GenePharma Co., Ltd (Shanghai, China). PI3K activity was assayed as previously described [15].

### Cell transfection

DNA vectors were transfected into cells using the Lipofectamine 3000 reagent (Invitrogen, CA, United States), according to the manufacturer's instructions. Briefly, LV-NC or LV-EGFR (Genechem, Shanghai, China) was introduced into cells when cell growth reached approximately 80% confluence. Cells were collected 48 h after transfection. Small interfering RNAs (siRNA) targeting UBE2R2-AS1 were synthesized by Sigma (Shanghai, China) and the sequences used are as follows: 5'-GACAUCUUCUGGUCAGAGATT-3'.

### Cell proliferation

HCC viability was assessed using Cell Counting Kit-8 as per the manufacturer's protocols. Briefly, ~5000 cells were seeded in 96 well plates, transfected for 48 h, and CCK-8 was added for 1 h. Absorbances were read at 450 nm.

### Invasiveness and migratory ability of HCC cells

Assays were performed in Boyden chambers with pore sizes of 8 µm in PET membranes. HCC cells were counted and accessed via transwell assays. After 48 h, noninvasive cells in the upper Matrigel membrane were removed with cotton-tipped swabs and cells in the bottom wells were fixed in methanol and toluidine blue stained. Cells were invasive when they passed through the lower membrane surface. All cells were imaged on an inverted light microscope (200 x magnifications) and quantified from three widefield images. Data shown are the averages of three independent experiments.

### Western blotting

RIPA buffer was used to lyse cells on ice for 15 min, after which a BCA assay was performed to quantify protein. Samples were then separated via SDS-PAGE and transferred to PVDF membranes that were then

blocked using 5% milk. Blots were probed overnight with primary antibodies (rabbit anti- $\beta$ -actin, ab179467, 1:5000; rabbit anti-MMP-7, ab207299; rabbit anti-AKT, ab8805; rabbit anti-EGFR, ab52894). Protein was detected via enhanced chemiluminescence (ECL, Millipore, MO, USA), with densitometry used to quantify protein levels.

### ***In vivo metastasis assays***

All animal experiments were carried out in Wuhan Servicebio Technology Development Co., Ltd., Wuhan, China, and were approved by the ethics committee of the Wuhan Servicebio Technology (-2018-05-09). In vivo assessments were performed in male nude mice aged 6 weeks (Beijing Vitonlihua Experimental Animal Technology Co. Ltd, Beijing, China). Animals were housed in specified cages that were approved by the national animal guidelines of our institute. For in vivo tumor growth,  $1 \times 10^6$  HCC cells were subcutaneously injected into the flanks of 5 mice from ( $n = 5$  for each group). The tumor volumes and weights were measured at the indicated time points. Five weeks following injection, mice were humanely killed by CO<sub>2</sub> in accordance with ethical study requirements. For in vivo metastatic growth in the lungs, mice were injected with indicated treated cells ( $4 \times 10^5$  cells, 5 mice per group) in the tail vein to produce the pulmonary metastasis model. Ten weeks following injection, mice were humanely killed by CO<sub>2</sub> in accordance with ethical study requirements and H&E stained to identify the presence of metastatic foci in the lungs. None anesthetics were used during animal experiments.

### ***RNA immunoprecipitation (RIP) assay***

A Magna RIP RNA-Binding Protein Immunoprecipitation Kit (Millipore, Bedford, MA, USA) was used to perform the RIP assay to evaluate the interaction between UBE2R2-AS1 and miR-302b in HCC cells and performed as previous.

### ***Luciferase reporter assay***

Luciferase reporter assays were performed as previous [16]. The target genes of LncUBE2R2-AS1

were predicted using three bioinformatics algorithms starBase 3.0 (<http://starbase.sysu.edu.cn/>). miR-302b was identified to be downregulated by LncUBE2R2-AS1, therefore the 3'-UTR of UBE2R2-AS1 containing miR-302b responsive element was cloned into pGL4.13 luciferase reporter vector (UBE2R2-AS1 wt-3' UTR). Luciferase mutant vector was obtained by mutating miR-302b binding site (UBE2R2-AS1 mut-3' UTR). The fragments of UBE2R2-AS1 comprising wild-type (WT) and mutant (MUT) miR-302b binding sites were designed and synthesized by Shanghai GenePharma. Luciferase activity was measured using a Dual-Luciferase Reporter Assay System (Promega Corporation). Renilla luciferase activity was used to normalize the data.

### ***Statistical analysis***

GraphPad Prism (GraphPad Software) was utilized for all statistical testing. Data are means  $\pm$  SEM. Data were tested using two-tailed Student's *t*-tests, one-way ANOVA followed by Tukey's post-hoc test, Wilcoxon signed-rank tests, Pearson chi-squared tests, Pearson correlation analyses, Log-rank tests, Fisher's exact tests, nonparametric Mann-Whitney *U* tests, and Cox proportional hazards regression models as appropriate, with  $p < 0.05$  as the significance threshold. All experiments were performed at least in triplicate.

## **Results**

### ***UBE2R2-AS1 was increased in HCC***

To identify UBE2R2-AS1 expressed in HCC tissues, we firstly performed qRT-PCR showed UBE2R2-AS1 was up-regulated in 182 HCC compared to adjacent normal tissues (Figure 1(a)). As shown in Figure 1(b), UBE2R2-AS1 was expressed more highly in stage III tissues than in stage I/II samples. Moreover, the expression of UBE2R2-AS1 in larger tumor size HCC ( $\geq 5$  cm) tissues was higher than that in smaller tumor size HCC ( $< 5$  cm) tissues (Figure 1(c)). Consistent with this result, RT-qPCR analysis result showed UBE2R2-AS1 expression level in HCC cell lines (Huh7,

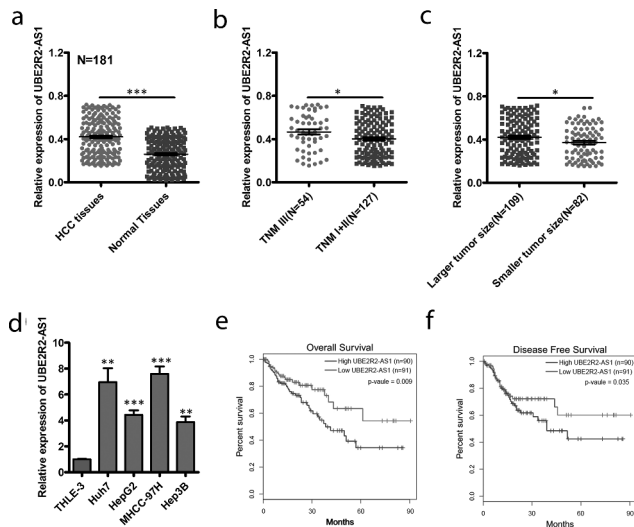


**Figure 1. UBE2R2-AS1 is increased in HCC and associated with poor survival.** (a) UBE2R2-AS1 in 181 paired HCCs and ANTs were examined by Realtime-PCR. (b) The expression of UBE2R2-AS1 was examined in different clinical stages of HCC samples by qRT-PCR. (c) The relative expression levels of UBE2R2-AS1 in the larger tumor size ( $\geq 5$  cm) and smaller tumor size ( $< 5$  cm) were determined by qRT-PCR. (d) UBE2R2-AS1 expression in HCC cell lines (Huh7, HepG2, MHCC-97H, and Hep3B) and normal cell (THLE-3). (e and f) Kaplan-Meier survival analyses were conducted to determine the overall survival rate (e) and disease-free survival rate (f). \* $P < 0.05$ ; \*\* $P < 0.01$ ; \*\*\* $P < 0.001$ .

HepG2, MHCC-97H, and Hep3B) was significantly upregulated compared with normal cell line (Figure 1(d)). These data suggested that the expression of UBE2R2-AS1 was increased in HCC tissues and cells.

### Increased UBE2R2-AS1 expression was correlated with poor survival in HCC

To further assess the clinical relevance of UBE2R2-AS1 expression in patients with HCC, we divided the 181 patient samples according to their levels of UBE2R2-AS1 expression (UBE2R2-AS1-high or UBE2R2-AS1-low;  $n = 90$  and  $91$ , respectively) based on the median UBE2R2-AS1 expression level in HCC tumor tissue samples. As shown in Table 1, Chi-squared tests were then used to compare clinical characteristics between groups, revealing that higher UBE2R2-AS1 levels were associated with a high AFP serum level ( $P = 0.003$ ), larger tumor size ( $P = 0.004$ ), multiple

of Tumor number ( $P = 0.043$ ), and advantaged TNM stage ( $P = 0.001$ ). In addition, in order to explore the interplay UBE2R2-AS1 between expression and prognosis in patients with HCC, we collected relevant follow-up data. Finally, we assessed the prognostic relevance of UBE2R2-AS1 in 181 HCC via a Kaplan-Meier approach, revealing a significant association between elevated UBE2R2-AS1 expression and reduced overall survival (OS) ( $p = 0.009$ , Figure 1(e)) as well as disease-free survival (DFS) ( $p = 0.035$ , Figure 1(f)), meaning that higher levels of this lncRNA are correlated with a worse prognosis. A multivariate analysis was additionally conducted to identify factors predictive of OS and DFS (Tables 2 and 3), revealing that elevated UBE2R2-AS1 expression independently predicted reduced OS (HR = 1.619, 95% CI: 1.241–2.738,  $p = 0.043$ ) and DFS (HR = 1.775, 95% CI: 1.244–2.728,  $p = 0.041$ ) in HCC patients. These results suggested that high UBE2R2-AS1 expression offers prognostic utility in HCC patients.

### Effects of UBE2R2-AS1 Knockdown on HCC cells growth and metastasis

To investigate the role of UBE2R2-AS1, we chose Huh7 and MHCC-97H cells which have a relative higher level of UBE2R2-AS1 for further experiments. Through shRNA, UBE2R2-AS1 expression was significantly decreased in these cell lines (Figure 2(a)). CCK8 assay showed UBE2R2-AS1 downregulation impaired the proliferation of Huh7 and MHCC-97H cells (Figure 2(b)). Next, cell migration and invasion were assessed by Transwell assay. Results showed that UBE2R2-AS1 knockdown reduced migration and invasion of Huh7 and MHCC-97H cells (Figure 2(c,d)). To verify the in vivo consequences of UBE2R2-AS1 knockdown, we injected Huh7-shNC and sh-UBE2R2-AS1 cells into the lateral tail vein of nude mice and evaluated both the metastatic growth in the lungs and the survival of the mice. Ten weeks post-injection, lungs were H&E stained and micro-metastases assessed (Figure 2(e)). Mice injected with Huh7-sh-UBE2R2-AS1 cells showed fewer numbers of metastatic foci which upon examination were of smaller size vs, the Huh7-shNC

**Table 2.** Univariate and multivariate analyses of overall survival (OS).

Variables	Univariate analysis of OS			Multivariate analysis of OS		
	HR	95% CI	p value	HR	95% CI	p value
Age (years) $\geq 55$ vs $< 55$	1.421	0.633–1.785	0.166	-	-	-
Gender Female vs Male	1.358	0.594–1.846	0.615	-	-	-
HBsAg Positive vs Negative	1.946	0.588–2.946	0.245	-	-	-
HBeAg Positive vs Negative	1.176	0.567–2.649	0.348	-	-	-
AFP, ng/ml $\geq 20$ vs $< 20$	1.719	1.186–2.885	0.018	0.682	0.328–1.899	0.355
HBV DNA, IU/ml $\geq 1000$ vs $< 1000$	1.038	0.589–1.684	0.768	-	-	-
Tumor size, cm $\geq 5$ vs $< 5$	1.748	1.379–2.965	0.028*	1.856	1.438–2.368	0.039*
Tumor number Multiple vs Single	1.802	1.278–3.122	0.013*	1.681	1.298–2.513	0.026*
Vascular invasion Present vs Absent	0.816	0.341–1.642	0.398	-	-	-
Tumor differentiation III–IV vs I–II	0.766	0.307–1.365	0.694	-	-	-
UBE2R2-AS1 level High vs Low	1.845	1.312–3.681	0.011*	1.619	1.241–2.738	0.043*

HR, hazard ratio; 95% CI, 95% confidence interval. \* P value  $< 0.05$ .

**Table 3.** Univariate and multivariate analyses of disease-free survival (DFS).

Variables	Univariate analysis of RFS			Multivariate analysis of DFS		
	HR	95% CI	p value	HR	95% CI	p value
Age (years) $\geq 55$ vs $< 55$	1.754	0.563–1.648	0.305	-	-	-
Gender Female vs Male	0.989	0.535–1.853	0.435	-	-	-
HBsAg Positive vs Negative	1.565	0.453–2.156	0.625	-	-	-
HBeAg Positive vs Negative	1.125	0.522–1.673	0.186	-	-	-
AFP, ng/ml $\geq 20$ vs $< 20$	1.354	0.846–1.348	0.348	-	-	-
HBV DNA, IU/ml $\geq 1000$ vs $< 1000$	1.889	1.267–2.043	0.022*	1.387	0.596–1.769	0.346
Tumor size, cm $\geq 5$ vs $< 5$	1.758	1.445–2.158	0.035*	1.835	1.068–2.164	0.022*
Tumor number Multiple vs Single	1.956	1.451–2.638	0.021*	1.719	1.145–2.867	0.038*
Vascular invasion Present vs Absent	1.453	0.351–1.877	0.835	-	-	-
Tumor differentiation III–IV vs I–II	1.687	0.486–1.643	0.854	-	-	-
UBE2R2-AS1 level High vs Low	1.854	1.452–3.053	0.013*	1.775	1.244–2.728	0.041*

HR, hazard ratio; 95% CI, 95% confidence interval. \* P value  $< 0.05$ .

group (Figure 2(f)). In addition, mice injected with sh-UBE2R2-AS1 cells had a significantly higher survival rate compared to shNC group (Figure 2(g)). Meanwhile, UBE2R2-AS1 knockdown was associated with delayed tumor formation and a significant reduction in tumor size in vivo (Figure 2(h,i)). Taken together, these results indicate that UBE2R2-AS1 was an oncogene in HCC.

### UBE2R2-AS1 controls MMP -7, and -9 expression via PI3K-AKT pathway in HCC

Next, we explored the underlying molecular mechanisms of the UBE2R2-AS1-mediated to enhance HCC progression. Interestingly, from the GEPIA (Gene Expression Profiling Interactive Analysis) data, we found that UBE2R2-AS1 was positively co-expression with MMP -7 and -9 from the respective (Figure 3(a)). Meanwhile, in HCC cells knock down UBE2R2-AS1, a marked decrease in MMP -7 and -9 mRNA and protein levels were observed (Figure 3(b,c)). In addition, the phosphorylation of AKT molecules was clearly inactivated in

both the HCC cell lines with UBE2R2-AS1 knock-down (Figure 3(d)). Following, HCC cells were transiently transfected with shUBE2R2-AS1, shNC, or pmyr-AKT, as described in the Methods section, and we found that the ectopic expression of AKT in shUBE2R2-AS1 cells significantly restored cell migration and invasion (Figure 3(e)), increased mRNA levels of MMP7 and MMP9 (Figure 3(f)). Kinase activity assays and Western blot assays further showed that PI3K, but not phosphatase and tensin homolog deleted on chromosome 10, was regulated by UBE2R2-AS1 (Figure 3(g,h)). Collectively, these results suggest that UBE2R2-AS1 played oncogene via PI3K-AKT pathway.

### UBE2R2-AS1-Mediated PI3K-AKT Signaling activation by EGFR

The activation of PI3K-AKT signaling is primarily mediated by the interactions between receptor tyrosine kinases (RTKs) and their specific ligands. Two different mitogens (EGF and hepatocyte growth factor [HGF]) were utilized to explore

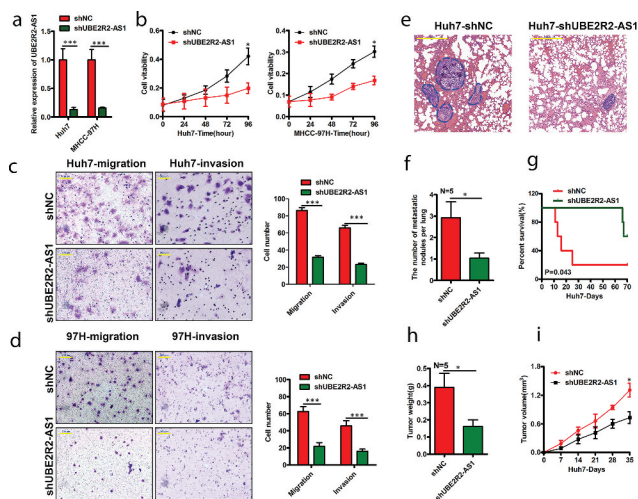


**Figure 2. Effects of UBE2R2-AS1 Knockdown on HCC cells growth and metastasis.** (a) RT-qPCR analysis of UBE2R2-AS1 expression in indicated HCC cells after the transfection of si-UBE2R2-AS1 or si-NC. (b) The proliferation of UBE2R2-AS1 deficient-Indicated HCC cell was detected using the Cell Counting Kit-8 assay. (c and d) Transwell assays were performed to assess the migratory and invasive abilities of Indicated HCC cells following si-UBE2R2-AS1 or si-NC transfection. (e) H & E staining of mouse lung tissues from indicated treated group. (f) Numbers of metastatic foci observed in each group (n = 5). (g) Comparisons of the OS curves of mice by Kaplan–Meier survival analyses. (h and i) Indicated treated HCC cells were subcutaneously injected into nude recipient mice (n = 5). \*P < 0.05; \*\*P < 0.01; \*\*\*P < 0.001.

whether RTKs are necessary for UBE2R2-AS1-mediated PI3K activation in the indicated HCC cell lines. From the GEPIA data indicated that EGFR, but not HGFR, was positively with UBE2R2-AS1 (Figure 4(a)). Meanwhile, in HCC cells knock down UBE2R2-AS1, a marked decrease in EGFR mRNA level instead of HGFR was observed (Figure 4(b)). As shown in Figure 4(c), UBE2R2-AS1 robustly inhibited AKT activation triggered by EGF in both indicated HCC cells compared with the corresponding control cells, but no such changes were observed in response to HGF stimulation (Figure 4(d)). Above results indicated that UBE2R2-AS1 active PI3K-AKT pathway depends on EGFR instead of HGFR. To explore whether UBE2R2-AS1 regulates HCC cells migration and invasion through EGFR, shNC, shUBE2R2-AS1, or UBE2R2-AS1+LV-EGFR was introduced into HCC cells. First, the efficiency of LV-EGFR transfection was verified using RT-qPCR. The data revealed that transfection with LV-EGFR resulted in a significant increase in

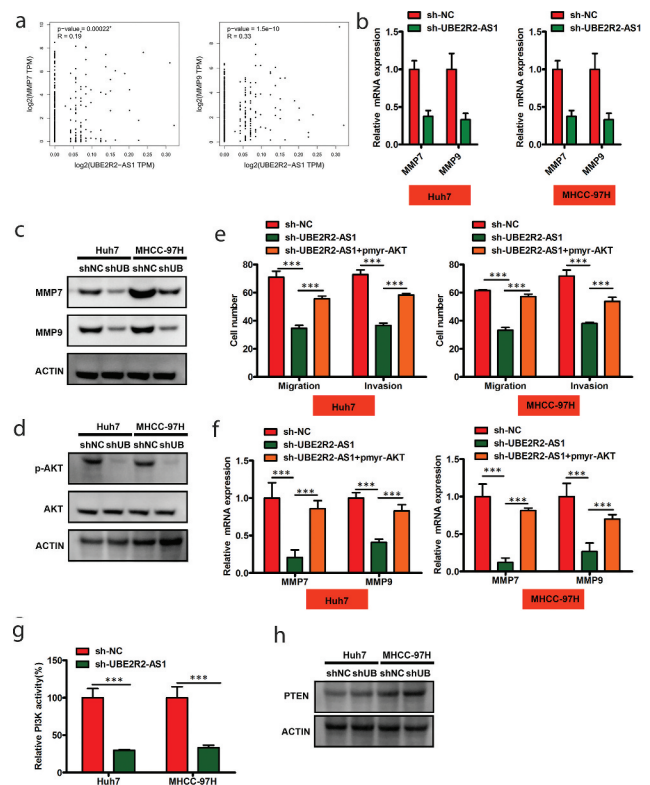


**Figure 3. UBE2R2-AS1 controls MMP –7, and –9 expression via PI3K-AKT pathway in HCC.** (a) GEPIA tool indicated that a strong positively correlation between the expression of UBE2R2-AS1 and MMP7 and 9 in these HCC tissue samples, respective. (b and c) MMP7 and 9 mRNA and protein level expression analysis in indicated HCC cells with UBE2R2-AS1 knock down. (d) The background total expression levels and phosphorylation levels of AKT (p-AKT) were analyzed by Western blotting in the indicated cell lysates. (e) HCC cells were transiently transfected with shNC, shUBE2R2-AS1 or pmyr-AKT. Transwell migration assay or the Matrigel invasion assay representative results are shown. (f) The relative mRNA expression levels of MMP-7and –9 were analyzed after the indicated treatments. (g) The PI3K kinase activity was determined. (h) The protein of PTEN was analyzed in indicated treated HCC cells. \*P < 0.05; \*\*P < 0.01; \*\*\*P < 0.001.

EGFR expression in HCC cells (Figure 4(e)). Furthermore, the decreased migration and invasion ability of HCC cells caused by EIF3J-AS1 knock down was reversed in HCC cells through up-regulated EGFR (Figure 4(f)). Taken together, UBE2R2-AS1-Mediated PI3K–AKT Signaling activation by EGFR.

### UBE2R2-AS1 sponged miR-302b to induce EGFR level in HCC

Following, we explored the mechanism that UBE2R2-AS1 regulated EGFR expression by

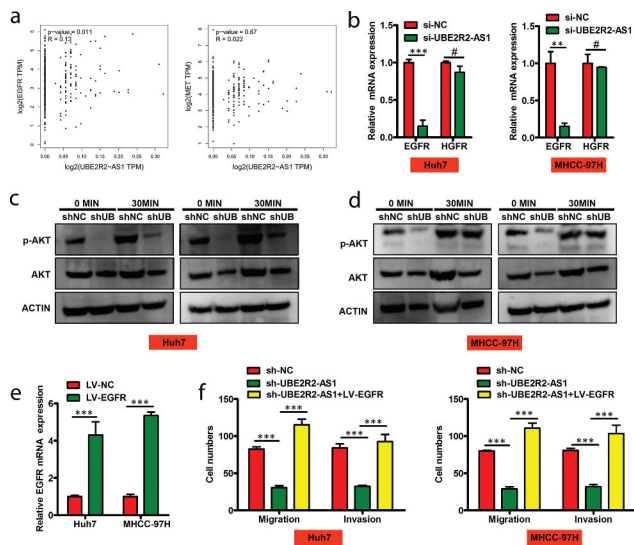


**Figure 4. UBE2R2-AS1-Mediated PI3K-AKT Signaling activation by EGFR.** (a) GEPIA tool indicated that a strong positive correlation between the expression of UBE2R2-AS1 and EGFR in these HCC tissue samples. (b) EGFR and HGFR mRNA expression analysis in indicated HCC cells with UBE2R2-AS1 knock down. (c and d) The indicated cell lines were exposed to EGF or HGF for 0 or 5 minutes and analyzed by Western blotting with the indicated antibodies. (e) EGFR mRNA was performed by RT-qPCR in indicated HCC cells. (f) Transwell assays were performed to assess the migratory and invasive abilities of indicated HCC cells. \*P < 0.05; \*\*P < 0.01; \*\*\*P < 0.001.

publicly available algorithm starBase 3.0 to predict the directly interacting miRNAs of UBE2R2-AS1. MiR-302b was found to share complementary binding sites with UBE2R2-AS1 (Figure 5(a)), and it was selected for further verification because this miRNA was reported to act as an oppressor during HCC progression [17]; more important was reported to target EGFR in HCC [18]. WT-UBE2R2-AS1 or MUT-UBE2R2-AS1 was transfected into indicated HCC cells in the presence of agomiR-302b or agomiR-NC to confirm this prediction. MiR-302b expression was significantly increased in HCC cells after transfection with agomiR-302b (Figure 5(b)). The luciferase activity of WT-UBE2R2-AS1 cells was drastically decreased after transfection with agomiR-302b in HCC cells; however, no changes in the activity of MUT-UBE2R2-AS1 were detected in the presence of miR-302b upregulation (Figure 5(c)). The interaction between miR-302b and UBE2R2-AS1 was further determined using RIP assay, and the data revealed that UBE2R2-AS1 and miR-302b were enriched in

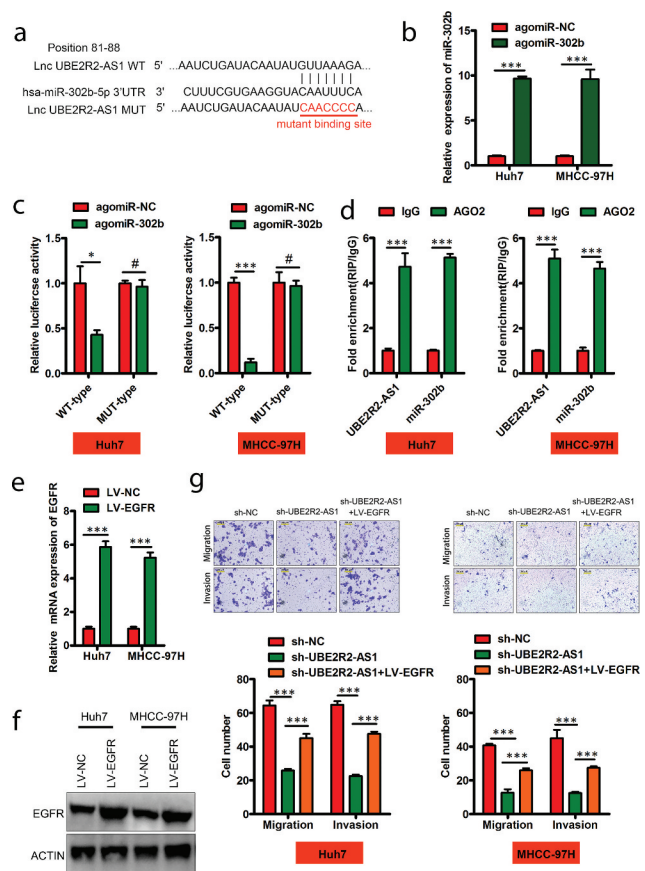


**Figure 5. UBE2R2-AS1 directly interacts with miR-302b in HCC as a molecular miRNA sponge to induce EGFR level.** (a) Bioinformatics analysis revealed the binding sites of miR-302b within UBE2R2-AS1. (b) miR-302b expression was performed by RT-qPCR. (c) Luciferase activity was performed in indicated HCC cell lines. (d) UBE2R2-AS1 and miR-302b were enriched in Ago2-containing immunoprecipitated compared with the IgG control. (e and f) EGFR mRNA and protein level was performed by RT-qPCR and WB. (g) Transwell assays were performed to assess the migratory and invasive abilities of indicated HCC cells. \*P < 0.05; \*\*P < 0.01; \*\*\*P < 0.001; P > 0.05.

Ago2-containing immunoprecipitates compared with that observed in the IgG control (Figure 5(d)). To explore whether UBE2R2-AS1 regulates EGFR expression through sponging miR-302b, si-UBE2R2-AS1 plus antagomiR-302b, or antagomiR-NC was introduced into HCC cells. First, the efficiency of antagomiR-302b transfection was verified using RT-qPCR and WB (Figure 5(e,f)). Furthermore, the downregulation of EGFR mRNA caused by knock down was reversed in HCC cells through antagomiR-302b re-introduction (Figure 5(g)). These results suggested that UBE2R2-AS1 positively regulated EGFR expression in HCC cells and this was achieved through sponging miR-302b.

## Discussion

As HCC causes large amounts of death, finding effective biomarkers and therapeutic targets for HCC is a pivot task [19]. Increasing evidences show lncRNAs play key roles in the progression of various cancers, including HCC [20–22]. Such as, LINC00461 enhanced HCC progression via miR-149-5p/LRIG2 axis [23]. LncRNA PVT1 played a key role in HCC cell autophagy [24]. LncRNA LASP1-AS significantly enhanced HCC malignant [25]. In the present study, we found that patient samples from individuals with HCC exhibited increased UBE2R2-AS1 expression, with a high AFP serum level, larger tumor size, multiple of tumor number, and advantaged TNM stage. This increase in UBE2R2-AS1 levels was also independently predictive of reduced OS and DFS, thus predicting poorer HCC patient outcomes. When we decreased the expression of UBE2R2-AS1 both in vitro and in vivo we were able to suppress the metastasis of HCC cells. These findings thus strongly suggested that UBE2R2-AS1 is a key oncogene of the metastatic progression of HCC, in addition to being a biomarker of advanced disease that can predict patient outcomes.

Previous studies indicated that the key process during tumor invasion is the enhanced proteolytic activity of cancer cell-expressed MMPs that mediate the degradation of the stroma of neighboring cells and enhance the spread of tumor cells [15]. MMP-7 is also known as matrilysin, and it cleaves many protein components of the ECMs [26]. MMP-7 was also found to be a direct target of miR-489 in HCC to enhance tumor cell migration and invasion in HCC. Previous studies indicated MMP-9 degrades the ECM, activates IL-1 $\beta$ , and cleaves several chemokines [27], could as played a major role in tumor angiogenesis, through its critical intervention in the regulation of growth plate angiogenesis and recruitment of endothelial stem cells [28]. Increased MMP-9 was associated with an advantaged TNM stage present of lymph node invasion, poor overall prognosis in HCC [29]. Combined with GEPIA and our studies showed that UBE2R2-AS1 was closely positively associated with MMP7/9 and EGFR level in HCC

tissues and knock down UBE2R2-AS1 leading MMP-7/9 and EGFR level down-regulated in HCC cell lines. Meanwhile, the downregulation of MMP -7 and -9 mRNA caused by UBE2R2-AS1 knock down was reversed in HCC cells through increasing EGFR. These findings suggested that UBE2R2-AS1 mediated its effects on HCC progression through MMP -7, and -9 by EGFR.

Amounts studies indicated that lncRNAs could interact with mRNA, proteins, or miRNAs to induce gene expression [30,31]. In multiple types of tumorigenesis, amounts studies indicated lncRNAs acted as competing endogenous RNAs (ceRNAs) for miRNAs [10,23,24]. Such as, in colorectal carcinoma obtained chemoresistance via KCNQ1OT1 enhancing ATG4B level through sponging miR-34 [32]. Besides, MALAT1 played a key role in cell stemness by enhancing Oct4 expression by sponging miR-20b-5p in colorectal carcinoma [33]. In addition, DGCR5 activated KLF1 to inhibit HCC progression via sponging miR-346 [4,34]. Following, we wonder whether UBE2R2-AS1 exerts roles through sponging miRNAs to regulate the EGFR level. First, miR-302b was predicted to share a complementary binding site for UBE2R2-AS1, and the interaction and binding between UBE2R2-AS1 and miR-302b were further confirmed using luciferase reporter and RIP assays. Second, UBE2R2-AS1 downregulation increased miR-302b expression and thereby resulted in a decrease in EGFR expression. Third, down-regulated miR-302b has been reported to be associated with enhancing HCC progression. Fourth, miR-302b has been reported to target EGFR in HCC [18].

Taken together, our findings revealed a ceRNA model including UBE2R2-AS1, miR-302b, and EGFR in HCC cells. Collectively, UBE2R2-AS1 overexpression promotes HCC development through regulating the MMP-7/9 axis via EGFR-PI3K-AKT pathway. Our research provides a new mechanism regulating HCC tumorigenesis. Our further study will focus on performing RNA-Seq experiment to explore more novelty targeted genes of UBE2R2-AS1.

## Disclosure statement

The authors declare that they have no competing interests.

## Funding

The study was funded by the Project of Shanghai Science and Technology Commission [7411960100].

## Availability of data and materials

All data generated and analyzed during this study are included in this published article.

## Authors' contributions

F-F Z conceived the study. J-H L wrote the manuscript. J-H L and J-S N designed and revised the manuscript. J-H L analyzed and interpreted the data. J-H L assisted in data analysis. All authors read and approved the final version of the manuscript.

## Ethics approval and consent to participate

The present study was approved by the Ethics Committee of the 900 Hospital of the Joint Logistics (Fuzhou, Fujian). Written informed consent was obtained from all patients prior to the study.

## References

- [1] Bray F, Ferlay J, Soerjomataram I, et al. Global cancer statistics 2018: GLOBOCAN estimates of incidence and mortality worldwide for 36 cancers in 185 countries. *CA Cancer J Clin.* 2018;68:394–424.
- [2] Chen W, Zheng R, Baade PD, et al. Cancer statistics in China, 2015. *CA Cancer J Clin.* 2016;66:115–132.
- [3] Altekruse SF, Henley SJ, Cucinelli JE, et al. Changing hepatocellular carcinoma incidence and liver cancer mortality rates in the United States. *Am J Gastroenterol.* 2014;109:542–553.
- [4] Si T, Chen Y, Ma D, et al. Transarterial chemoembolization prior to liver transplantation for patients with hepatocellular carcinoma: A meta-analysis. *J Gastroenterol Hepatol.* 2017;32:1286–1294.
- [5] Donato L, Scimone C, Alibrandi S, et al. Transcriptome analyses of lncRNAs in A2E-stressed retinal epithelial cells unveil advanced links between metabolic impairments related to oxidative stress and retinitis pigmentosa. *Antioxidants (Basel).* 2020;9. DOI:10.3390/antiox9050435
- [6] Yan X, Hu Z, Feng Y, et al. Comprehensive genomic characterization of long non-coding RNAs across human cancers. *Cancer Cell.* 2015;28:529–540.
- [7] Wang KC, Chang HY. Molecular mechanisms of long noncoding RNAs. *Mol Cell.* 2011;43:904–914.
- [8] Mercer TR, Dinger ME, Mattick JS. Long non-coding RNAs: insights into functions. *Nat Rev Genet.* 2009;10:155–159.
- [9] Leucci E, Vendramin R, Spinazzi M, et al. Melanoma addiction to the long non-coding RNA SAMMSON. *Nature.* 2016;531:518–522.
- [10] Wang YG, Wang T, Shi M, et al. Long noncoding RNA EPB41L4A-AS2 inhibits hepatocellular carcinoma development by sponging miR-301a-5p and targeting FOXL1. *J Exp Clin Cancer Res.* 2019;38:153.
- [11] Wang Y, Yang L, Chen T, et al. A novel lncRNA MCM3AP-AS1 promotes the growth of hepatocellular carcinoma by targeting miR-194-5p/FOXA1 axis. *Mol Cancer.* 2019;18:28.
- [12] Jin S, Yang X, Li J, et al. p53-targeted lincRNA-p21 acts as a tumor suppressor by inhibiting JAK2/STAT3 signaling pathways in head and neck squamous cell carcinoma. *Mol Cancer.* 2019;18:38.
- [13] Xu W, Hu GQ, Da Costa C, et al. Long noncoding RNA UBE2R2-AS1 promotes glioma cell apoptosis via targeting the miR-877-3p/TLR4 axis. *Onco Targets Ther.* 2019;12:3467–3480.
- [14] Zheng H, Yang Y, Han J, et al. TMED3 promotes hepatocellular carcinoma progression via IL-11/STAT3 signaling. *Sci Rep.* 2016;6:37070.
- [15] Zheng H, Yang Y, Hong YG, et al. Tropomodulin 3 modulates EGFR-PI3K-AKT signaling to drive hepatocellular carcinoma metastasis. *Mol Carcinog.* 2019;58:1897–1907.
- [16] Donato L, Scimone C, Rinaldi C, et al. Stargardt phenotype associated with two ELOVL4 promoter variants and ELOVL4 downregulation: new possible perspective to etiopathogenesis. *Invest Ophthalmol Vis Sci.* 2018;59:843–857.
- [17] Wang L, Yao J, Zhang X, et al. miRNA-302b suppresses human hepatocellular carcinoma by targeting AKT2. *Mol Cancer Res.* 2014;12:190–202.
- [18] Wang L, Yao J, Shi X, et al. MicroRNA-302b suppresses cell proliferation by targeting EGFR in human hepatocellular carcinoma SMMC-7721 cells. *BMC Cancer.* 2013;13:448.
- [19] Raoul JL, Forner A, Bolondi L, et al. Updated use of TACE for hepatocellular carcinoma treatment: how and when to use it based on clinical evidence. *Cancer Treat Rev.* 2019;72:28–36.
- [20] Liu Y, Li J, Li F, et al. SNHG15 functions as a tumor suppressor in thyroid cancer. *J Cell Biochem.* 2019;120:6120–6126.
- [21] Dong H, Hu J, Zou K, et al. Activation of lncRNA TINCR by H3K27 acetylation promotes Trastuzumab resistance and epithelial-mesenchymal transition by targeting MicroRNA-125b in breast cancer. *Mol Cancer.* 2019;18:3.
- [22] Zhu P, Wang Y, Wu J, et al. lncBRM initiates YAP1 signalling activation to drive self-renewal of liver cancer stem cells. *Nat Commun.* 2016;7:13608.

- [23] Ji D, Wang Y, Li H, et al. Long non-coding RNA LINC00461/miR-149-5p/LRIG2 axis regulates hepatocellular carcinoma progression. *Biochem Biophys Res Commun.* **2019**;512:176–181.
- [24] Yang L, Peng X, Jin H, et al. Long non-coding RNA PVT1 promotes autophagy as ceRNA to target ATG3 by sponging microRNA-365 in hepatocellular carcinoma. *Gene.* **2019**;697:94–102.
- [25] Yin L, Chen Y, Zhou Y, et al. Increased long noncoding RNA LASP1-AS is critical for hepatocellular carcinoma tumorigenesis via upregulating LASP1. *J Cell Physiol.* **2019**;234:13493–13509.
- [26] Yokoyama Y, Grunebach F, Schmidt SM, et al. Matrilysin (MMP-7) is a novel broadly expressed tumor antigen recognized by antigen-specific T cells. *Clin Cancer Res.* **2008**;14:5503–5511.
- [27] Opendakker G, Van den Steen PE, Dubois B, et al. Gelatinase B functions as regulator and effector in leukocyte biology. *J Leukoc Biol.* **2001**;69:851–859.
- [28] Heissig B, Hattori K, Dias S, et al. Recruitment of stem and progenitor cells from the bone marrow niche requires MMP-9 mediated release of kit-ligand. *Cell.* **2002**;109:625–637.
- [29] Sun SJ, Wang N, Sun ZW, et al. MiR-5692a promotes the invasion and metastasis of hepatocellular carcinoma via MMP9. *Eur Rev Med Pharmacol Sci.* **2018**;22:4869–4878.
- [30] Zhu P, Wang Y, Huang G, et al. lnc-beta-Catm elicits EZH2-dependent beta-catenin stabilization and sustains liver CSC self-renewal. *Nat Struct Mol Biol.* **2016**;23:631–639.
- [31] Guo D, Oho AUID, Li Y, et al. DANCR promotes HCC progression and regulates EMT by sponging miR-27a-3p via ROCK1/LIMK1/COFILIN1 pathway. *Cell Prolif.* **2019**;52:e12628.
- [32] Li Y, Li C, Li D, et al. lncRNA KCNQ1OT1 enhances the chemoresistance of oxaliplatin in colon cancer by targeting the miR-34a/ATG4B pathway. *Onco Targets Ther.* **2019**;12:2649–2660.
- [33] Tang D, Yang Z, Long F, et al. Long noncoding RNA MALAT1 mediates stem cell-like properties in human colorectal cancer cells by regulating miR-20b-5p/Oct4 axis. *J Cell Physiol.* **2019**;234:20816–20828.
- [34] Wang YG, Liu J, Shi M, et al. LncRNA DGCR5 represses the development of hepatocellular carcinoma by targeting the miR-346/KLF14 axis. *J Cell Physiol.* **2018**;234:572–580.